

The dependence of test-mass coating and substrate thermal noise on beam shape in the advanced Laser Interferometer Gravitational-Wave Observatory (advanced LIGO)

Geoffrey Lovelace

Theoretical Astrophysics, California Institute of Technology, Pasadena, California 91125

(Dated: February 18, 2019)

In second-generation, ground-based interferometric gravitational-wave detectors such as the Advanced Laser Interferometer Gravitational-Wave Observatory (advanced LIGO), the dominant noise at frequencies $f \sim 40$ Hz to ~ 200 Hz is expected to be due to thermal fluctuations in the mirrors' substrates and coatings which induce random fluctuations in the shape of the mirror face. The laser-light beam averages over these fluctuations; the larger the beam and the flatter its light-power distribution, the better the averaging and the lower the resulting thermal noise. This has led O'Shaughnessy and Thorne to propose flattening and enlarging the beam shape to reduce the thermal noise. In this paper I derive and discuss simple scaling laws that describe the dependence of the thermal noise (which includes Brownian and thermoelastic noises in the mirrors' coatings and substrates) on the beam's (axisymmetric) light-power distribution. Each of these scaling laws has previously been deduced, from somewhat general arguments rather than detailed calculations, by O'Shaughnessy; independently, the same scaling laws have been found by Vyatchanin [for Brownian coating noise], by O'Shaughnessy, Strigin and Vyatchanin [for substrate thermoelastic noise], and by Vinet [for substrate Brownian noise]. These scaling laws are valid in the limit that the mirror dimensions are large compared to the beam radius. Recently Agresti has computed the sensitivity improvement when flat-top (or "mesa") beams are used instead of gaussian beams (with the diffraction loss fixed). When the mirror substrate is fused silica with radius not larger than the baseline radius for advanced LIGO (17 cm), the coating-noise infinite-mirror scaling laws agree with Agresti's finite-mirror calculations within about 10%, and the substrate-noise infinite-mirror scaling laws agree with Agresti's finite-mirror calculations within about 15%.

PACS numbers: 04.80.Nn

I. INTRODUCTION AND SUMMARY

A. Motivation

The advanced interferometers in the Laser Interferometer Gravitational-Wave Observatory (advanced LIGO) will be approximately ten times more sensitive than the current LIGO interferometers, leading to an improvement in event rate such that the first few hours of advanced LIGO will contain more signals than the entire year-long science run that is presently under way [1]. In advanced LIGO's most sensitive frequency band ($f \sim 40$ to 200 Hz), the sensitivity is limited by internal thermal noise, i.e., by noise in the substrates and reflective coatings of the four test masses (see, e.g., Fig. 1 of Ref. [2]). Lowering the internal thermal noise would increase advanced LIGO's event rate throughout that band.

Internal thermal noise can be divided into two different types: *Brownian thermal noise* (due to imperfections in the substrate or coating material, which couple normal modes of vibration to each other) and *thermoelastic noise* (due to random flow of heat in the substrate or coating, which causes random thermal expansion). When the laser beam shape is gaussian, the Brownian and thermoelastic noises in the substrate (e.g. [3]) and in the coating (e.g. [4][5]) are well understood. One way of lowering the internal thermal noise is to flatten the shape of the laser beam that measures the test mass position so that it better averages over the mirror faces' fluctuating

shapes [6, 7]. O'Shaughnessy, Strigin, and Vyatchanin [8] have numerically quantified the resulting reduction in substrate thermoelastic noise, and Agresti [2] and Agresti and DeSalvo [9, 10] have done the same for other thermal noises.

These promising results highlight the importance of understanding deeply the relationship between the beam shape and the internal thermal noises. To this end, it is useful to ask whether there is a simple relation between the beam shape and thermal noise for *any* beam shape. O'Shaughnessy [11] and Vyatchanin [12] have addressed this question by proposing a relation for Brownian coating thermal noise; in particular, they deduced that the beam shape and coating thermal noise are related by a simple scaling law, provided the beam is sufficiently small compared to the mirror—i.e. for a mirror idealized as having arbitrarily large diameter and thickness. In parallel with the research reported here, O'Shaughnessy has also applied his argument to the cases of coating thermoelastic, substrate Brownian, and substrate thermoelastic noise [11]; the derivation for the substrate thermoelastic scaling law has previously appeared in work by O'Shaughnessy, S. Strigin, and Vyatchanin [8]. Vinet [13] has found the substrate Brownian scaling law.

In this article, building on the work described above, I flesh out the relation between all four types of internal thermal noise and beam shape. Specifically, I verify O'Shaughnessy's and Vyatchanin's scaling law for both Brownian and thermoelastic coating noise. Also, I show that similar scaling laws can be written down for Brown-

ian and thermoelastic substrate noise. These simple scaling laws make it straightforward to estimate the change in the internal thermal noise caused by changing the shape of the laser beam. I also estimate the errors that result from finite mirror size.

B. Model and Summary

To explore the effect of the beam shape on the internal thermal noise, I consider a cylindrical test mass substrate of radius R and thickness H and suppose that these size scales are comparable: $R \sim H$. I choose a cylindrical coordinate system (r, φ, z) such that $r = 0$ is the mirror axis, $z = 0$ is the reflectively coated surface of the mirror substrate, and points with $0 < z < H$ are inside the mirror substrate.

An axisymmetric laser beam with intensity profile $p(r)$ is normally incident on the mirror¹. The intensity profile is normalized, so

$$2\pi \int_0^R dr r p(r) = 1. \quad (1)$$

The beam measures $q(t)$, a weighted average of the mirror's longitudinal position $Z(r, \varphi, t)$ (Eq. (3) of Ref. [14])

$$q(t) \equiv \int_0^{2\pi} d\varphi \int_0^R dr r p(r) Z(r, \varphi, t). \quad (2)$$

In LIGO, so as to keep diffraction losses $\lesssim 1$ ppm, the beam radius over which, say, 95% of the signal $q(t)$ is collected, is kept significantly smaller than the mirror radius R and thickness H . This motivates the idealization of the mirror as a semi-infinite slab bounded by a plane, $R \rightarrow \infty$, $H \rightarrow \infty$. (The accuracy of this infinite-test-mass (ITM) approximation will be discussed in Sec. IV B.)

Internal thermal noise will cause small fluctuations in the longitudinal position of the mirror $Z(r, \varphi, t)$. The spectral density S associated with the measurement of the mirror position q is given by the fluctuation dissipation theorem (Eq. (1) of Ref. [14]):

$$S_q = \frac{2k_B T}{\pi^2 f^2} \frac{W_{\text{diss}}}{F^2}. \quad (3)$$

Here k_B is Boltzmann's constant, T is the temperature of the material, and W_{diss} is the power that would be dissipated if a longitudinal force F with frequency

f and pressure distribution $p(r)$ were applied to the mirror surface (Levin's [14] thought experiment). Because the frequencies of interest (i.e. $f \sim 100$ Hz) are far below the lowest resonant frequencies of the mirror $f_{\text{res}} \sim (\text{a few km/s})/(\text{about } 10 \text{ cm}) \sim 10^4$ Hz, the hypothetical applied force F can be idealized as static when computing the resulting strain of the mirror.

Thus the noise S_q can be computed using the following algorithm:

1. Statically deform the (semi-infinite) mirror with a force F with pressure distribution $p(r)$ the same as the light's intensity profile;
2. compute the Brownian and thermoelastic dissipated power W_{diss} due to the deformation caused by F ;
3. substitute W_{diss} into Eq. (3) to get the spectral density S_q of the thermal noise of a measurement of the average position q .

Note that from S_q , one can easily compute the thermally-induced gravitational-wave-strain noise power $S_h(f)$ of a measurement of the advanced LIGO interferometer. If mirrors 1 and 2 are in one arm (of length $L = 4$ km), and mirrors 3 and 4 are in the other arm (also of length L), advanced LIGO measures $h \equiv [(q_1 - q_2) - (q_3 - q_4)]/L$, where $q_{1,2,3,4}$ are the measured positions of the four mirrors. Because the noises in the four test masses are uncorrelated, the spectral density S_h is just $S_h = (4/L^2)S_q$. In the remainder of this article, when referring to the noise of a single test mass, the subscript "q" will be suppressed (i.e. $S \equiv S_q$), while the gravitational-wave-strain noise power will always be referred to as S_h .

In Sec. II, I compute the strain distribution that results from applying the force F to a homogeneous, isotropic, semi-infinite mirror with a very thin reflective coating of a possibly different material. The calculation is a straightforward generalization of Sec. 2 of Ref. [4]. In this calculation, I model the coating as a thin layer (of order microns, as compared to the cm size scales of the substrate) which adheres to the mirror surface. In Sec. III I use the strain distributions to compute each of the four types of thermal noise $S(f)$.

In Levin's thought experiment, the dissipation associated with Brownian thermal noise can be modeled as arising from a loss angle, which is an imaginary (i.e. damping) correction to the material's Young's modulus caused by coating or substrate imperfections. Following Harry and collaborators [4], in Sec. III I introduce two loss angles in the coating: ϕ_{\parallel} (for damping due to deformations that are in the plane of the coating) and ϕ_{\perp} (for damping due to deformations normal to the plane of the coating). The loss angles themselves are taken to be constants; they do not depend on the deformation itself.

These losses, combined with the strain in the coating due to the static applied force F , yield W_{diss} [Eq. (21)],

¹ The shape of the mirror faces must also be changed slightly (by height changes \lesssim one wavelength of the laser light) so that $p(r)$ is an eigenmode of the arm cavity. In this paper, I assume that the mirror faces take whatever shape is necessary to support a beam with intensity profile $p(r)$.

which I then insert back into Eq. (3) to obtain for coating Brownian noise

$$S_{\text{coat}}^{\text{BR}} = C_{\text{coat}}^{\text{BR}} \int_0^\infty dr r p^2(r) = C_{\text{coat}}^{\text{BR}} \int_0^\infty dk k \tilde{p}^2(k) \quad (4)$$

[Eq. (22)]. Here $C_{\text{coat}}^{\text{BR}}$ does not depend on the beam shape, and $\tilde{p}(k)$ is (up to factors of 2π) the two-dimensional Fourier transform of $p(r)$ over the surface of the mirror:

$$\begin{aligned} \tilde{p}(k) &= \int_0^\infty dr r J_0(kr) p(r), \\ p(r) &= \int_0^\infty dk k J_0(kr) \tilde{p}(k). \end{aligned} \quad (5)$$

Here $J_0(x)$ is the 0th Bessel function of the first kind (the axisymmetry allows the 2D Fourier transform to reduce to a 1D Hankel transform). Equation (4) is the same scaling law that O’Shaughnessy [11] and Vyatchanin [12] have suggested for Brownian coating thermal noise.

In Levin’s thought experiment, the dissipation associated with thermoelastic noise arises from heat flow down temperature gradients, which are induced by compression of the coating or substrate by the force F . The increase in entropy corresponds to a dissipated power.

Braginsky and Vyatchanin ([5]) and Fejer and collaborators ([15]) have independently calculated the thermoelastic coating noise for gaussian beam shapes. When one scrutinizes their calculations, one can also read off the noise for generic beam shapes. The analyses in Appendix B.2 of Ref. [5] and in Sec. IV D of Ref. [15] both imply the following scaling law for thermoelastic coating noise [Eq. (27)]:

$$S_{\text{coat}}^{\text{TE}} = C_{\text{coat}}^{\text{TE}} \int_0^\infty dk k \tilde{p}^2(k). \quad (6)$$

Note that *the thermoelastic and Brownian coating noises obey the same scaling law.*

The substrate Brownian noise $S_{\text{sub}}^{\text{BR}}$ can be computed using essentially the same calculation as for the Brownian coating noise. Only one loss angle ϕ is needed to characterize the substrate’s imperfections, since the substrate is taken to be semi-infinite. From the strain in the substrate due to the static applied force F , it is straightforward to compute the scaling law for the substrate Brownian noise [Eq. (35)]:

$$S_{\text{sub}}^{\text{BR}} = C_{\text{sub}}^{\text{BR}} \int_0^\infty dk k \tilde{p}^2(k). \quad (7)$$

This law is also a trivial consequence of equations written down by Vinet (Eqs. (1) – (2) of Ref. [13]).

In the substrate, the heat flow is adiabatic, so the diffusion of heat has a negligible influence on the temperature distribution in Levin’s thought experiment. This leads to the following scaling law for the thermoelastic substrate noise [Eq. (37)]:

$$S_{\text{sub}}^{\text{TE}} = C_{\text{sub}}^{\text{TE}} \int_0^\infty dk k^2 \tilde{p}^2(k). \quad (8)$$

O’Shaughnessy, Strigin, and Vyatchanin [8] have previously derived this scaling law.

Combining all four results, I find that if $p_1(u)$ and $p_2(k)$ are two different beam shapes, then

$$\frac{S_{1,n}}{S_{2,n}} = \frac{\int_0^\infty dk k^n [\tilde{p}_1(k)]^2}{\int_0^\infty dk k^n [\tilde{p}_2(k)]^2} \quad (9)$$

where $n = 1$ for coating Brownian and coating thermoelastic noise, $n = 0$ for substrate Brownian noise, and $n = 2$ for substrate thermoelastic noise. If one knows $S_{1,n}$, computing $S_{2,n}$ amounts to computing simple integrals of $\tilde{p}(k)$. If one holds everything else fixed but changes the beam shape, Eq. (9) makes it straightforward to determine the improvement in the thermal noises, which implies an improvement in sensitivity for advanced LIGO.

In the remainder of this paper, I derive these scaling laws, comment on their implications for advanced LIGO, and estimate their accuracy for finite test masses. First, in Sec. II, I compute the strain S_{ij} due to a hypothetical applied force F with pressure distribution $p(r)$. In Sec. III, I compute the dissipated power W_{diss} for the Brownian and thermoelastic dissipation in the coating and the substrate, and insert W_{diss} into Eq. (3) to determine how the noise depends on the beam shape. In Sec. IV A, I discuss implications of this result for advanced LIGO, and in Sec. IV B I discuss the accuracies of the infinite-test-mass (ITM) scaling laws by comparing with others’ finite-test-mass (FTM) predictions for the cases of gaussian and flat-top (or “mesa”) beam shapes. I make some concluding remarks in Sec. V.

II. STRAIN OF A SEMI-INFINITE BODY WITH THIN FACIAL COATINGS DUE TO A STATIC, AXISYMMETRIC FORCE

The thermal noise is determined by the symmetric part of the strain S_{ij} that the test mass would experience if a normal force with pressure $p(r)$ were applied to the mirror surface. In this section, I evaluate S_{ij} in the mirror substrate and coating. In Sec. III, I use these results to compute W_{diss} [which, by Eq. (3), determines the thermal noise].

If the displacement vector of an element of the test mass is u_i , then the strain S_{ij} is $S_{ij} = \nabla_j u_i$. Following the methods developed in Ref. [16] (but correcting some typographical errors), Eq. (19) of Ref. [3] gives the cylindrical components of the displacement of the test mass

substrate:

$$u_r = \frac{1}{2\mu} \int_0^\infty dk J_1(kr) e^{-kz} \left(1 - \frac{\lambda + 2\mu}{\lambda + \mu} + kz \right) \tilde{p}(k), \quad (10a)$$

$$u_\varphi = 0, \quad (10b)$$

$$u_z = \frac{1}{2\mu} \int_0^\infty dk J_0(kr) e^{-kz} \left(1 + \frac{\mu}{\lambda + \mu} + kz \right) \tilde{p}(k). \quad (10c)$$

Here λ and μ are the Lamé coefficients of the substrate. The vector u_i satisfies the equilibrium equation $\nabla_j T_{ij} = 0$. (Throughout this paper, I use the Einstein summation convention.)

The non-vanishing components of the symmetric part of the strain are [with commas denoting partial derivatives]

$$\theta = S_{ii}, \quad (11a)$$

$$S_{rr} = u_{r,r} = \theta - S_{zz} - S_{\varphi\varphi}, \quad (11b)$$

$$S_{\varphi\varphi} = \frac{u_r}{r}, \quad (11c)$$

$$S_{(rz)} = S_{(zr)} = \frac{1}{2}(u_{r,z} + u_{z,r}), \quad (11d)$$

$$S_{zz} = u_{z,z}. \quad (11e)$$

Evaluating the derivatives of Eqs. (10a) – (10c) and inserting the result into Eqs. (11a) – (11e) gives

$$\theta = \frac{1}{2\mu} \int_0^\infty dk k J_0(kr) \left(\frac{-2\mu}{\lambda + \mu} \right) e^{-kz} \tilde{p}(k), \quad (12a)$$

$$S_{rr} = \theta - S_{zz} - S_{\varphi\varphi}, \quad (12b)$$

$$S_{\varphi\varphi} = \frac{1}{2\mu} \int_0^\infty dk \frac{J_1(kr)}{r} e^{-kz} \left(1 - \frac{\lambda + 2\mu}{\lambda + \mu} + kz \right) \tilde{p}(k), \quad (12c)$$

$$S_{(zr)} = -\frac{1}{2\mu} \int_0^\infty dk k J_1(kr) (kz) e^{-kz} \tilde{p}(k), \quad (12d)$$

$$S_{zz} = \frac{1}{2\mu} \int_0^\infty dk k J_0(kr) \left(-\frac{\mu}{\lambda + \mu} - kz \right) e^{-kz} \tilde{p}(k). \quad (12e)$$

Setting $z = 0$ in Eqs. (12a)–(12e) and combining with Eq. (5) yields the nonvanishing stresses on the substrate surface:

$$\theta|_{z=0} = \left(\frac{-1}{\lambda + \mu} \right) p(r), \quad (13a)$$

$$S_{rr}|_{z=0} = \frac{1}{2} \left(\frac{-1}{\lambda + \mu} \right) p(r) - S_{\varphi\varphi}|_{z=0}, \quad (13b)$$

$$S_{\varphi\varphi}|_{z=0} = \frac{1}{2} \left(\frac{-1}{\lambda + \mu} \right) \int_0^\infty dk \frac{J_1(kr)}{r} \tilde{p}(k), \quad (13c)$$

$$S_{zz}|_{z=0} = \frac{1}{2} \left(\frac{-1}{\lambda + \mu} \right) p(r). \quad (13d)$$

Here I have used the identity

$$\int_0^\infty dk k J_0(kr) J_0(kr') = \frac{\delta(r' - r)}{r'}. \quad (14)$$

Note that on the surface of the substrate θ and S_{zz} are *local* [i.e. their values at any point depend only on the value of $p(r)$ at that point], while $S_{\varphi\varphi}$ is *nonlocal*. The component S_{rr} can be written as the sum of a local part and a non-local part; the non-local part of S_{rr} is just $-S_{\varphi\varphi}$.

The thin coating approximation gives the nonvanishing components of the coating strain in terms of the strain on the substrate surface (Eq. (A4) of Ref. [4]):

$$\theta^{\text{coat}} = \frac{\lambda + 2\mu_{\text{coat}}}{\lambda_{\text{coat}} + 2\mu_{\text{coat}}} (\theta - S_{zz})|_{z=0} + \frac{\lambda + 2\mu}{\lambda_{\text{coat}} + 2\mu_{\text{coat}}} S_{zz}|_{z=0}, \quad (15a)$$

$$S_{rr}^{\text{coat}} = S_{rr}|_{z=0} = \theta^{\text{coat}} - S_{\varphi\varphi}^{\text{coat}} - S_{zz}^{\text{coat}}, \quad (15b)$$

$$S_{\varphi\varphi}^{\text{coat}} = S_{\varphi\varphi}|_{z=0}, \quad (15c)$$

$$S_{zz}^{\text{coat}} = \frac{\lambda - \lambda_{\text{coat}}}{\lambda_{\text{coat}} + 2\mu_{\text{coat}}} (\theta - S_{zz})|_{z=0} + \frac{\lambda + 2\mu}{\lambda_{\text{coat}} + 2\mu_{\text{coat}}} S_{zz}|_{z=0}. \quad (15d)$$

In Ref. [4], these conditions are said to hold in the limit that the Poisson ratio of the substrate and coating are “not too different,” but this restriction is unnecessary (see Appendix B).

Finally, after inserting Eqs. (13a) – (13d) into Eqs. (15a) – (15d) I conclude that θ^{coat} and S_{zz}^{coat} are *local*; while $S_{\varphi\varphi}^{\text{coat}}$ and S_{rr}^{coat} are *nonlocal*. However, this non-locality turns out *not* to influence the coating noises. This is because, after using Eq. (15b) to eliminate S_{rr}^{coat} , it turns out that the remaining non-local part $S_{\varphi\varphi}^{\text{coat}}$ only appears in the coating W_{diss} [Eqs. (21) and (26)] via the integral

$$\begin{aligned} & \int_0^\infty dr r S_{(ij)}^{\text{coat}} S_{(ij)}^{\text{coat}} \\ &= \int_0^\infty dr r \left[(S_{rr}^{\text{coat}})^2 + (S_{\varphi\varphi}^{\text{coat}})^2 + (S_{zz}^{\text{coat}})^2 \right] \\ &= \int_0^\infty dr r \left[(\theta^{\text{coat}} - S_{zz}^{\text{coat}})^2 + (S_{zz}^{\text{coat}})^2 \right. \\ & \quad \left. + 2(S_{\varphi\varphi}^{\text{coat}})^2 - 2S_{\varphi\varphi}^{\text{coat}} (\theta^{\text{coat}} - S_{zz}^{\text{coat}}) \right]. \end{aligned} \quad (16)$$

In Appendix A, I show that

$$\int_0^\infty dr r (S_{\varphi\varphi}^{\text{coat}})^2 - S_{\varphi\varphi}^{\text{coat}} (\theta^{\text{coat}} - S_{zz}^{\text{coat}}) = 0, \quad (17)$$

so only the local parts of the strain (θ^{coat} and S_{zz}^{coat}) influence the thermal noise. This fact turns out to imply local coating scaling laws in agreement with O’Shaughnessy’s [11] and Vyatchanin’s [12] arguments (Sec. III).

III. INTERNAL THERMAL NOISE

A. Brownian coating noise

For Brownian thermal noise in an elastic material, the dissipated power is [Eq. (12) of Ref. [14] with a static applied force and with $U = -(1/2)S_{ij}T_{ij}$]

$$W_{\text{diss}} = -\pi f \int_0^d dz \int_0^{2\pi} d\varphi \int_0^\infty dr r \phi(f) S_{ij} T_{ij}. \quad (18)$$

Here ϕ is the loss angle (i.e., the imaginary, damping part of the Young's modulus of the coating material) and T_{ij} is the stress. When the material is the thin reflective coating of a mirror, there are effectively *two* loss angles [4], ϕ_{\parallel} and ϕ_{\perp} , defined so that in the previous equation

$$\begin{aligned} & \phi(f) S_{ij} T_{ij} \\ \rightarrow & \phi_{\parallel}(f) (S_{rr}^{\text{coat}} T_{rr}^{\text{coat}} + S_{\varphi\varphi}^{\text{coat}} T_{\varphi\varphi}^{\text{coat}}) + \phi_{\perp}(f) S_{zz}^{\text{coat}} T_{zz}^{\text{coat}} \\ = & \phi_{\parallel}(f) S_{ij}^{\text{coat}} T_{ij}^{\text{coat}} + (\phi_{\perp} - \phi_{\parallel}) S_{zz}^{\text{coat}} T_{zz}^{\text{coat}}. \end{aligned} \quad (19)$$

This result can be obtained by combining Eqs. (4) and (13) – (15) of Ref. [4] with Eq. (9) of Ref. [14] and recalling that in the coating, the strain is diagonal [Eqs. (15a) – (15d)].

For a homogeneous coating, the stress T_{ij}^{coat} is

$$T_{ij}^{\text{coat}} = -\lambda^{\text{coat}} \theta^{\text{coat}} \delta_{ij} - 2\mu^{\text{coat}} S_{(ij)}^{\text{coat}}, \quad (20)$$

where λ^{coat} and μ^{coat} are the Lamé coefficients of the coating, $S_{(ij)}^{\text{coat}}$ is the symmetric part of the coating strain, and $\theta \equiv S_{ii}$ is the expansion. Combining Eqs. (19), (18) and (20) gives the following expression for W_{diss} :

$$\begin{aligned} W_{\text{diss}} &= 2\pi^2 f d \phi_{\parallel}(f) \int_0^\infty dr r A \\ &\quad + 2\pi^2 f d [\phi_{\perp}(f) - \phi_{\parallel}(f)] \int_0^\infty dr r B, \\ A &= (\lambda^{\text{coat}} \theta_{\text{coat}}^2 + 2\mu^{\text{coat}} S_{(ij)}^{\text{coat}} S_{(ij)}^{\text{coat}}), \\ B &= S_{zz}^{\text{coat}} (\lambda^{\text{coat}} \theta^{\text{coat}} + 2\mu^{\text{coat}} S_{zz}^{\text{coat}}). \end{aligned} \quad (21)$$

Combining Eqs. (21), (15a) – (15d), (13a) – (13d), and (17) and then inserting the result into Eq. (3) gives the spectral density S of the Brownian coating noise. However, for the present purpose, only terms involving the beam shape are relevant. Absorbing all other terms into a single constant $C_{\text{coat}}^{\text{BR}}$ yields

$$S_{\text{coat}}^{\text{BR}} = C_{\text{coat}}^{\text{BR}} \int_0^\infty dr r p^2(r). \quad (22)$$

This is a local scaling law; i.e., the noise at each point on the mirror's surface is proportional to the square of the beam intensity there. This law is the same as O'Shaughnessy's [11] and Vyatchanin's [12] scaling law for the Brownian coating thermal noise.

Parseval's equation [which follows from Eq. (5)] makes it easy to rewrite this scaling law in the Fourier domain, which will facilitate comparison with the substrate noise. The result is

$$S_{\text{coat}}^{\text{BR}} = C_{\text{coat}}^{\text{BR}} \int_0^\infty dk k \tilde{p}^2(k). \quad (23)$$

B. Thermoelastic Coating Noise

The calculation of the thermoelastic coating noise is similar to the calculation of Brownian coating noise. But now, in response to the static, normal applied pressure $p(r)$, the dissipated power W_{diss} is caused by heat flow, $\propto \nabla \delta T$, down a temperature gradient $\nabla \delta T$ caused by the material's deformation:

$$W_{\text{diss}} = \frac{\pi \kappa}{T} \int_0^\infty dz \int_0^\infty dr r (\nabla \delta T)^2. \quad (24)$$

[Eq. (5) of Ref. [3] in the case of a static applied force and after evaluating the time average and trivial φ integral]. Here T is the temperature of the coating in the absence of the deformation and κ is the material's coefficient of thermal conductivity.

Braginsky and Vyatchanin [5] and Fejer and collaborators [15] have independently solved for the thermoelastic coating noise. The results obtained in Ref. [5] are correct only when the coating and substrate have the same elastic properties (Sec. I in Ref. [15]); however, this restriction is not relevant here, since Refs. [15] and [5] agree on the coating thermoelastic noise's dependence on the beam shape $p(r)$.

If the temperature change were adiabatic, δT would simply be proportional to θ^{coat} (see, e.g., Eq. (12) of Ref. [3]). (Physically, this simply means that the temperature of an element in the coating changes linearly with volume.) However, as noted in Ref. [5], the diffusive heat characteristic length ℓ_D of the substrate and coating (on the order of mm) is far larger than the coating thickness d (which is on the order of a few microns). Because diffusive heat flow in the longitudinal direction is *not* negligible, heat flow in the direction normal to the coating cannot be treated adiabatically [5]. By contrast, the *substrate* thermoelastic noise *can* be treated adiabatically (Sec. IIID), as can the heat flow in the plane of the coating (“tangential” heat flow).

Because the tangential heat flow is adiabatic, $\partial \delta T / \partial r \sim \theta / w$, where $w \sim \text{cm}$ is the length scale over which $p(r)$ varies. On the other hand, $\partial \delta T / \partial z \sim \theta / \ell_D$, where $\ell_D \sim \text{mm}$ is the diffusive heat characteristic length. Because the tangential derivatives are much smaller than the longitudinal derivatives, all derivatives except $\partial / \partial z$ may be neglected. It follows that W_{diss} will depend only on $p(r)$ and not on its radial derivatives.

Based on these observations, Braginsky and Vyatchanin [5] and Fejer and collaborators [15] solve the thermoconductivity equation (e.g., Eq. (1) of Ref. [15])

for the temperature perturbations δT . Combining Eqs. (B5) – (B7), (66), and (68) of Ref. [15] [or equivalently, combining Eqs. (B.10) and (B.12) of Ref. [5] with Eqs. (13a) and (15a)] shows that the temperature perturbations in the coating have the form

$$\delta T \propto p(r) \times F(z), \quad (25)$$

where $F(z)$ is a function of z only. (The precise form of $F(z)$ is given in Refs. [5] and [15] but is not needed in the present discussion.)

Next, Braginsky and Vyatchanin compute the squared gradient $(\nabla \delta T)^2 \simeq (\partial \delta T / \partial z)^2$ in Eq. (24) to obtain W_{diss} ; Fejer and collaborators instead compute W_{diss} by considering the interaction of i) the *unperturbed* stress and strain [i.e., the stress and strain due to $p(r)$ when temperature perturbations are neglected], and ii) the (complex) *perturbations* of the stress and strain caused by the small temperature perturbations δT . Both methods lead to the following expression for W_{diss} : (Eqs. (B.13) and (B.10) of Ref. [5]; Eq. (69) of Ref. [15])

$$W_{\text{diss}} = \text{const} \times \int_0^\infty dr r p^2(r). \quad (26)$$

Plugging this result into Eq. (3) gives the scaling law

$$S_{\text{coat}}^{\text{TE}} = C_{\text{coat}}^{\text{TE}} \int_0^\infty dr r p^2(r) = C_{\text{coat}}^{\text{TE}} \int_0^\infty dk k \tilde{p}^2(k). \quad (27)$$

This is the same scaling law as for Brownian coating thermal noise. The coating thermoelastic noise is local and is the same as O’Shaughnessy’s [11] and Vyatchanin’s [12] law for Brownian coating thermal noise.

C. Brownian Substrate Noise

For Brownian substrate thermal noise there is only one relevant loss angle, ϕ , so the dissipated power is (Eq. (49)

of Ref. [3] with a static applied force)

$$W_{\text{diss}} = 2\pi^2 f \phi(f) \int_0^\infty dz \int_0^\infty dr r (\lambda \theta^2 + 2\mu S_{(ij)} S_{(ij)}). \quad (28)$$

The integral of the squared strain can be expanded as

$$\begin{aligned} & \int_0^\infty dz \int_0^\infty dr r S_{(ij)} S_{(ij)} \\ &= \int_0^\infty dz \int_0^\infty dr r (S_{rr}^2 + S_{\varphi\varphi}^2 + S_{zz}^2) \\ &= \int_0^\infty dz \int_0^\infty dr r [(\theta - S_{zz})^2 + S_{zz}^2 + 2S_{(rz)}^2 \\ &\quad + 2S_{\varphi\varphi}^2 - 2S_{\varphi\varphi}(\theta - S_{zz})]. \end{aligned} \quad (29)$$

In Appendix A, I show that

$$\int_0^\infty dr r [S_{\varphi\varphi}^2 - S_{\varphi\varphi}(\theta - S_{zz})] = 0. \quad (30)$$

Substituting this result into Eq. (29) yields

$$\begin{aligned} W_{\text{diss}} &= 2\pi^2 f \phi(f) \int_0^\infty dz \int_0^\infty dr r [\lambda \theta^2 + 2\mu (\theta - S_{zz})^2 \\ &\quad + 2\mu S_{zz}^2 + 4\mu S_{(rz)}^2]. \end{aligned} \quad (31)$$

This expression can be evaluated term by term. Inserting Eq. (12a) into the integral of θ^2 gives

$$I_\theta \equiv \int_0^\infty dz \int_0^\infty dr r \theta^2 = \frac{1}{4\mu^2} \left(\frac{2\mu}{\lambda + \mu} \right)^2 \int_0^\infty dk k \tilde{p}(k) \int_0^\infty dk' k' \tilde{p}(k') \int_0^\infty dz e^{-(k+k')z} \int_0^\infty dr r J_0(kr) J_0(k'r). \quad (32)$$

Using the identity

$$\int_0^\infty dr r J_n(kr) J_n(k'r) = \frac{\delta(k - k')}{k} \quad (33)$$

on Eq. (32) and evaluating the integral over z yields

$$I_\theta = \frac{1}{8\mu^2} \left(\frac{2\mu}{\lambda + \mu} \right)^2 \int_0^\infty dk k \tilde{p}^2(k). \quad (34)$$

The other terms in Eq. (31) can be evaluated similarly; they all turn out to have the same dependence on $\tilde{p}(k)$ as

I_θ . Inserting this result for W_{diss} into Eq. (3) gives the scaling law

$$S_{\text{sub}}^{\text{BR}} = C_{\text{sub}}^{\text{BR}} \int_0^\infty dk k \tilde{p}^2(k). \quad (35)$$

This scaling law is the same as the scaling law for the coating thermal noise [Eq. (23)] except that the z integration has reduced the power of k in the integrand by one. This scaling law agrees with Eqs. (1) – (2) of Ref. [13].

D. Thermoelastic Substrate Noise

In contrast to the case of coating thermoelastic noise, the substrate thermoelastic noise *can* be treated using the adiabatic approximation. Therefore, the temperature perturbations δT that drive the substrate thermoelastic noise $S_{\text{sub}}^{\text{TE}}$ are proportional to the expansion, i.e. $\delta T \propto \theta$. This implies (e.g., by Eq. (24), or Eq. (13) of Ref. [3])

$$S_{\text{sub}}^{\text{TE}} = C_{\text{sub}}^{\text{TE}} \int_0^\infty dz \int_0^\infty dr r (\nabla \theta)^2 \quad (36)$$

with $C_{\text{sub}}^{\text{TE}}$ independent of the strain (and thus also the beam shape). Inserting Eq. (12a) into Eq. (36) gives the scaling law; after absorbing all constants into $C_{\text{sub}}^{\text{TE}}$, it takes the form

$$S_{\text{sub}}^{\text{TE}} = C_{\text{sub}}^{\text{TE}} \int_0^\infty dk k^2 \tilde{p}^2(k), \quad (37)$$

which O’Shaughnessy, Strigin, and Vyatchanin obtain in Ref. [8]. This scaling law is the same as the scaling law for the substrate Brownian noise [Eq. (35)] except that the gradient raises the power of k by two.

IV. INFINITE-TEST-MASS (ITM) SCALING LAWS

To illustrate the scaling laws (22), (27), (35), and (37), suppose that the noise $S_{\tau,k}$ [with beam shape $p_k(r)$ and thermal noise type τ] is known. Here and throughout the remainder of this article, τ is a label that takes one of the following values: coating Brownian (Coat BR), coating thermoelastic (Coat TE), substrate Brownian (Sub BR), or substrate thermoelastic (Sub TE).

Now, if the beam shape were changed to $p_u(r)$ [while holding everything² else fixed], then the unknown noise $S_{\tau,u}$ [with beam shape $p_u(r)$] would be [Eq. (9)]:

$$S_{\tau,u} = C_{\text{ITM}}^2[\tau; p_u, p_k] S_{\tau,k}, \quad (38)$$

with

$$C_{\text{ITM}}^2[\tau; p_u, p_k] \equiv \frac{\int_0^\infty dk k^{n(\tau)} \tilde{p}_u^2(k)}{\int_0^\infty dk k^{n(\tau)} \tilde{p}_k^2(k)} \quad (39)$$

and

$$n(\tau) \equiv \begin{cases} 1 & : \tau = \text{Coat BR or Coat TE} \\ 0 & : \tau = \text{Sub BR} \\ 2 & : \tau = \text{Sub TE} \end{cases} \quad (40)$$

When the beam shape is changed from p_k to p_u , the amplitude sensitivity changes by a factor of $C_{\text{ITM}}[\tau; p_u, p_k]$.

² Since here I am neglecting edge effects, “everything” means the temperature, the materials’ elastic and thermal properties, the coating thickness, and the frequency. In Sec. IV B, when edge effects are considered, it will be the diffraction loss, not the mirror size, that is held fixed.

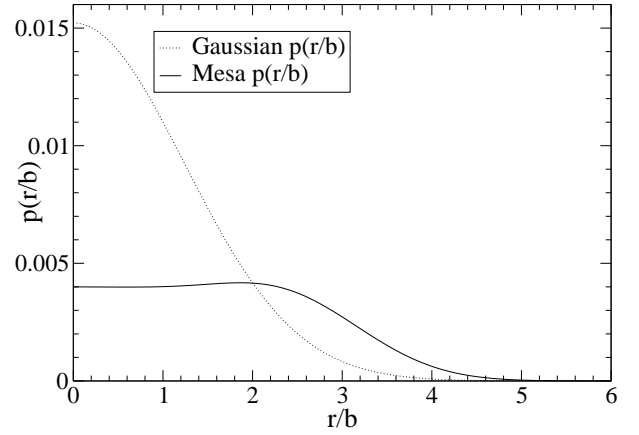


FIG. 1: A plot of $p_{\text{gauss}}(r/b)$ and $p_{\text{mesa}}(r/b)$ for beams with 1 ppm diffraction losses (in the clipping approximation) on a mirror with radius $R = 17$ cm. Here $b = \sqrt{L\lambda/2\pi} = 2.6$ cm is the width of the smallest Gaussian beam that can resonate in a LIGO arm cavity with length $L = 4$ km and light wavelength $\lambda = 1064$ nm.

A. Implications for advanced LIGO

In advanced LIGO, the thermal noise may be significantly reduced by changing the shape of the laser beam. One proposal is to replace the gaussian beam shape with a mesa beam (also called a flat-top beam) [7]. O’Shaughnessy, Strigin, and Vyatchanin [8] have calculated the resulting reduction in substrate thermoelastic noise, Vinet has done the same for substrate Brownian thermal noise [13] and Agresti [2] and Agresti and DeSalvo [9, 10] have done the same for both substrate and coating thermal noises—all for the realistic case of finite mirrors. The reduction in thermal noise can also be understood as a consequence of the simple ITM scaling laws derived above. Although I only compare gaussian and flat-top beams here, the scaling law given in Eq. (9) makes it simple—if one neglects finite-test-mass (FTM) effects—to compute the relative change in sensitivity for any two beam shapes.

The normalized gaussian beam shape is

$$p_{\text{gauss}}(w; r) = \frac{e^{-r^2/w^2}}{\pi w^2} \quad (41)$$

where w is the width of the gaussian beam. It is straightforward to compute $\tilde{p}_{\text{gauss}}(w; k)$, since the integral can be done analytically; the result is

$$\tilde{p}_{\text{gauss}}(w; k) = \int_0^\infty dr r J_0(kr) \frac{e^{-r^2/w^2}}{\pi w^2} = \frac{1}{2\pi} e^{-k^2 w^2/4}. \quad (42)$$

In position space, the mesa beam can be written as

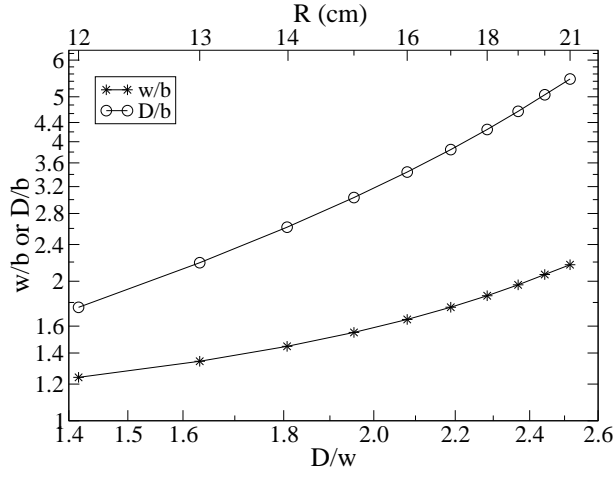


FIG. 2: A log-log plot of the gaussian beam-width parameter w and mesa beam-width parameter D as a function of mirror radius R (top of figure), for mirrors with 1 ppm diffraction loss in the clipping approximation. The ratio D/w is shown on the bottom of the figure. The parameter b is defined in Fig. 1.

(Eq. (2.5) of Ref. [6])

$$p_{\text{mesa}}(D; r) = N \left| 2\pi \int_0^D dr' r' \exp \left[-\frac{(r^2 + r'^2)(1-i)}{2b^2} \right] \right. \\ \left. \times I_0 \left[\frac{rr'(1-i)}{b^2} \right] \right|^2. \quad (43)$$

Here D is a measure of the width of the beam, $b \equiv \sqrt{\lambda L/2\pi}$, with $L = 4$ km the arm length and $\lambda = 1064$ nm the wavelength of the laser beam's primary frequency, and N is a normalization constant adjusted so Eq. (1) is satisfied. Note that $p_{\text{mesa}}(r)$ must be evaluated numerically; to compute $\tilde{p}(k)$, I use the Fast Hankel Transform algorithm [17].

Examples of the gaussian and mesa shapes are plotted in Fig. 1. In Fig. 2, the width parameters w and D of a sequence³ of gaussian and mesa beams are plotted as a function of mirror radius R for beams with 1 ppm of diffraction loss in the clipping approximation⁴. The ratio D/w is also shown on the bottom horizontal axis. It is sometimes useful to regard D and w (for 1 ppm losses) as functions of D/w rather than of R — with D/w actually being a surrogate for R .

The following three cases use Eqs. (38) – (40) to illustrate how the thermal noise in advanced LIGO changes

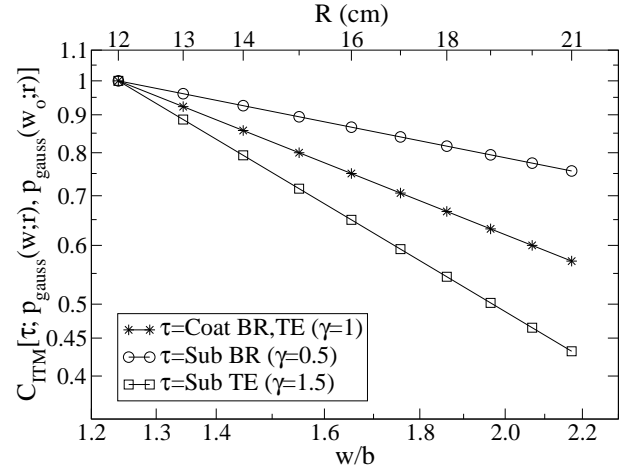


FIG. 3: The scaling of thermal noises with beam width w for gaussian beams in the infinite-test-mass (ITM) approximation. More specifically: a log-log plot of $C_{\text{ITM}}[\tau; p_{\text{gauss}}(w; r), p_{\text{gauss}}(w_o; r)]$ as a function of w/b . Here $w_o/b = 1.24$, which corresponds to $R = 12$ cm and 1 ppm diffraction losses. Each curve is a power law obeying $C \propto 1/w^\gamma$.

with different choices of gaussian and mesa beam shapes.

1. Noise of a resized gaussian beam

Suppose $p_k(r) = p_{\text{gauss}}(w_o; r)$. Then the thermal noises for a gaussian beam of some different size w are determined by evaluating $C_{\text{ITM}}[\tau; p_{\text{gauss}}(w; r), p_{\text{gauss}}(w_o; r)]$ [Eq. (39)] and inserting the result into Eq. (38). In this well-known case (see, e.g., the discussion and references in Ref. [10]), C_{ITM} can be evaluated analytically, yielding the following relation:

$$C_{\text{ITM}}^2[\tau; p_{\text{gauss}}(w; r), p_{\text{gauss}}(w_o; r)] \propto \frac{1}{w^{n(\tau)+1}}. \quad (44)$$

In Fig. 3, $C_{\text{ITM}}[\tau; p_{\text{gauss}}(w; r), p_{\text{gauss}}(w_o; r)]$ is plotted as a function of the beam width w .

2. Noise of a resized mesa beam

Suppose $p_k(r) = p_{\text{mesa}}(D_o; r)$. Then the thermal noises for a mesa beam of some different size D are determined by evaluating $C_{\text{ITM}}[\tau; p_{\text{mesa}}(D; r), p_{\text{mesa}}(D_o; r)]$ [Eq. (39)] and inserting the results into Eq. (38). As shown in Fig. 4, in this case C_{ITM} does not scale as an exact power of D (although the actual relations are very well approximated by power laws).

³ This particular sequence was chosen to facilitate comparison with the results of Ref. [10], which includes edge effects.

⁴ In the clipping approximation, the diffraction loss is simply $2\pi \int_R^\infty dr r p(r)$, where R is the mirror radius. In the ITM approximation, R is larger than all other length scales; however, the actual, finite value of R must be used in the clipping approximation for the diffraction loss to be nonvanishing.

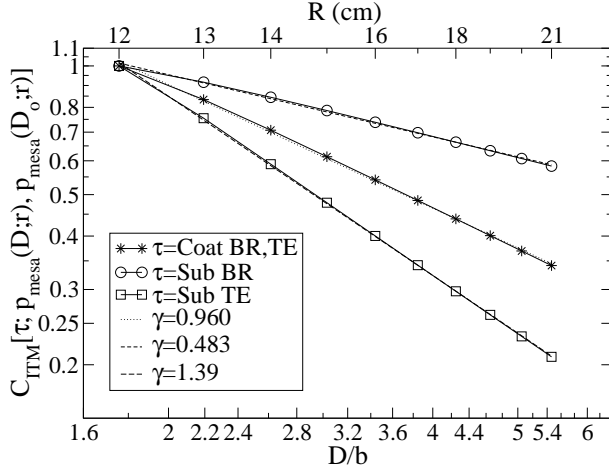


FIG. 4: The scaling of thermal noises with beam-width parameter D for mesa beams in the infinite-test-mass approximation. More specifically: a log-log plot of $C_{\text{ITM}}[\tau; p_{\text{mesa}}(D; r), p_{\text{mesa}}(D_o; r)]$ as a function of D/b . Here $D_o/b = 1.76$, which corresponds to a mirror radius of 12 cm and 1 ppm diffraction losses. The curves are well approximated by power laws of the form $C \propto 1/D^\gamma$.

3. Noise reduction by switching from a gaussian beam to a mesa beam with the same diffraction loss and mirror radius

Finally, Eq. (38) can be used to estimate the reduction in thermal noise by switching from a gaussian beam to a mesa beam that has the same clipping-approximation diffraction loss on a mirror of the same radius.

Two complications in the resized-beam scalings are not present when scaling from gaussian to mesa beams. First, while the original and resized beams were associated with different-sized mirrors, now the gaussian and mesa beams are associated with the *same* mirror. Second, when relating the gaussian and mesa beams, there is no need to specify a fiducial beam size (i.e. there is no analog of w_o and D_o). Without these two complications, the gaussian-to-mesa scaling is perhaps conceptually cleaner than the resized-beam scalings.

Figure 5 shows $C_{\text{ITM}}[\tau; p_{\text{mesa}}(D; r), p_{\text{gauss}}(w; r)]$ for the sequence of beams shown in Fig. 2 (beams with 1 ppm diffraction loss in mirrors of the same radius R). The relative improvement in amplitude sensitivity increases monotonically with the mirror radius R , or equivalently, with D/w ; however, when edge effects (finite-test-mass effects) are included, there is a limit to how much the sensitivity can be improved (Sec. IV B).

B. Errors due to neglecting finite-test-mass (FTM) effects

In the previous section, the ITM scaling laws predicted that, if the diffraction losses are held fixed, then the coating and substrate noises decrease monotonically with in-

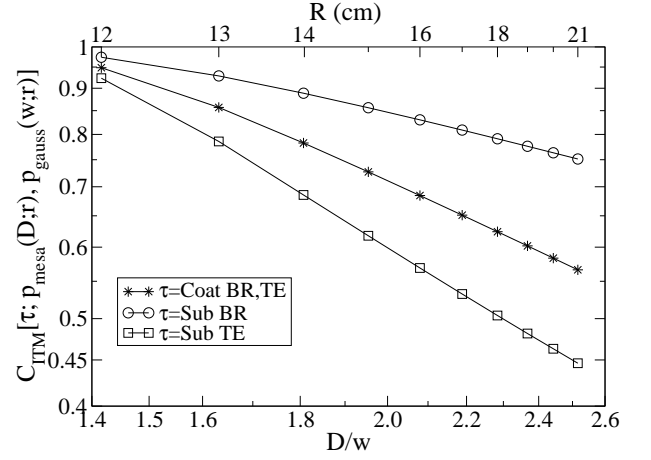


FIG. 5: The improvement in amplitude sensitivity when mesa beams are used instead of gaussian beams. More specifically: a log-log plot of $C_{\text{ITM}}[\tau; p_{\text{mesa}}(D; r), p_{\text{gauss}}(w; r)]$ as a function of D/w . For each mirror radius R , w and D are chosen so that the diffraction losses are 1 ppm in the clipping approximation.

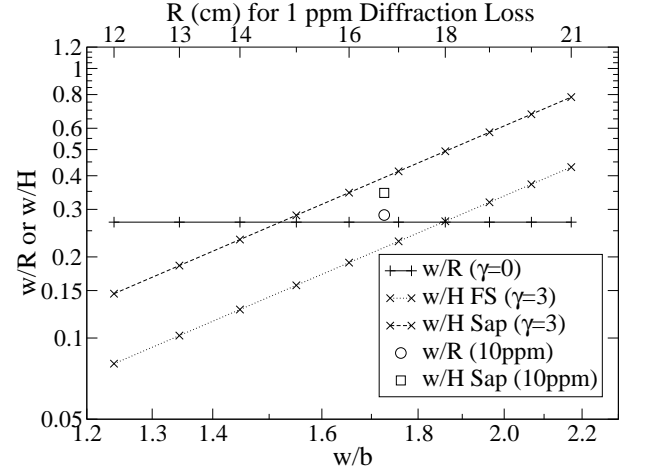


FIG. 6: How the gaussian beam width parameter w compares to the mirror radius R and thickness H , when i) the radius R is fixed so the clipping-approximation diffraction loss is 1 ppm (unless a 10 ppm loss is indicated), and ii) the thickness H is then determined by holding the mass at 40 kg, the advanced-LIGO baseline mirror mass. Each curve is proportional to w^γ . FS and Sap mean fused-silica and sapphire substrates.

creasing beam width [Figs. 3, 4, and 5]. In other words, for a given diffraction loss, the optimal beam width is simply “as large as possible.”

However, this conclusion is only as strong as the ITM approximation. Its validity can be checked by comparing the beam widths to the corresponding mirror dimensions. In our modeling, the mirror radii R are adjusted to maintain a constant clipping-approximation diffraction loss (CADL) [Fig. 2], while the thicknesses H is then determined by requiring the mirror mass be 40 kg—the design specification for Advanced LIGO. (Thus H will depend on whether the substrate is Fused Silica (FS) or sapphire

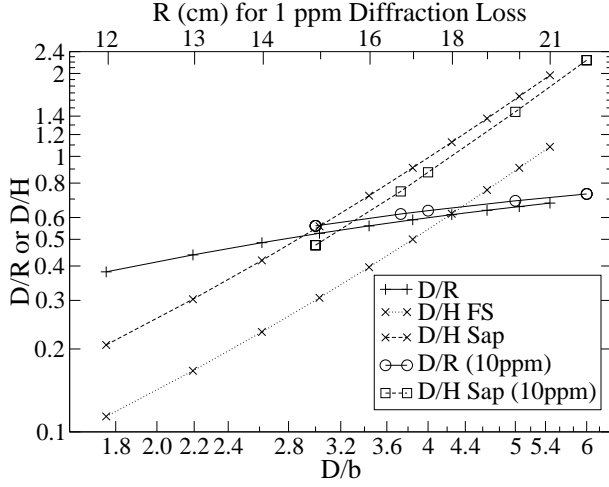


FIG. 7: How the mesa beam width parameter D compares to the mirror radius R and thickness H , when i) the radius R is fixed so the clipping-approximation diffraction loss is 1 ppm (unless a 10 ppm loss is indicated), and ii) the thickness H is then determined by holding the mass at 40 kg. The mirror radius R for 1 ppm losses is shown on the top axis; the 10 ppm mirror radii are (from left to right) $R^{10 \text{ ppm}} = 13.94$ cm, 15.7 cm, 16.37 cm, 18.85 cm, and 21.36 cm. FS and Sap mean fused-silica and sapphire substrates.

(Sap), since the densities of these materials differ by a factor of about 2.)

As shown in Figs. 6 and 7, for the sequences of beam widths considered in Sec. IV A, w and D can approach or even exceed H while simultaneously being significant fractions of the R . Consequently, edge effects (finite test-mass effects) may significantly change the sensitivity scalings depicted in Figs. 3, 4, and 5.

To estimate the importance of these edge effects, I compare the results in Secs. IV A 1 – IV A 3 to the finite-test-mass (FTM) results⁵ of Agresti and DeSalvo [10] (all types of thermal noise, 1 ppm CADL) and O’Shaughnessy, Strigin, and Vyatchanin [8] (substrate thermoelastic noise only, 10 ppm CADL). Specifically, from these data I read off the ratio

$$C_{\text{FTM}}[\tau; p_u(r), p_k(r)] \equiv \sqrt{\frac{S_{\tau,u}^{\text{FTM}}}{S_{\tau,k}^{\text{FTM}}}}. \quad (45)$$

This change in sensitivity can be compared to $C_{\text{ITM}}[\tau; p_k(r), p_u(r)]$, the change in sensitivity obtained by the ITM approximation. Specifically, if

$$\Delta[\tau; p_u(r), p_k(r)] \equiv \frac{C_{\text{FTM}}[\tau; p_u(r), p_k(r)]}{C_{\text{ITM}}[\tau; p_u(r), p_k(r)]}, \quad (46)$$

⁵ The FTM data used here assume that the coating extends all the way to the edge of the substrate face. In advanced-LIGO, the coating radius will actually be several mm smaller than the substrate radius (the baseline substrate radius for advanced LIGO is 170 mm).

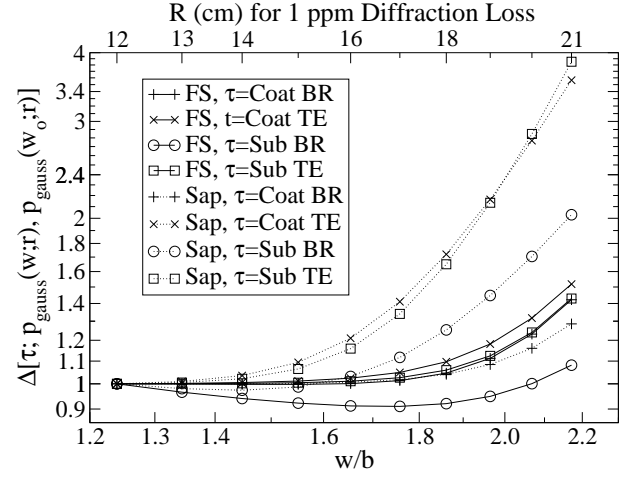


FIG. 8: A log-log plot of $\Delta[\tau; p_{\text{gauss}}(w; r), p_{\text{gauss}}(w_o; r)]$. The fractional error of the sensitivity change made by neglecting edge effects is $|1 - \Delta|$. Here $w_o/b = 1.24$, which corresponds to $R = 12$ cm and 1 ppm diffraction losses. The FTM values are obtained by taking ratios of the noises calculated by Agresti and DeSalvo [10]. FS and Sap mean fused-silica and sapphire substrates.

then $|1 - \Delta|$ is the fractional error made by using the ITM approximation to compute $C[\tau; p_u(r), p_k(r)]$.

In the following subsections, I consider the errors $|1 - \Delta|$ made [Secs. IV A 1 – IV A 3] by neglecting FTM effects.

1. Resized gaussian beam

Figure 8 plots $\Delta[\tau; p_{\text{gauss}}(w; r), p_{\text{gauss}}(w_o; r)]$ for mirror substrates made of fused silica, the baseline material for advanced LIGO mirrors [1]. For comparison, the figure also shows the corresponding values of Δ for sapphire substrates.

When the substrate is fused silica, the ITM and FTM scaling laws agree to better than about 10% so long as $R \lesssim 17$ cm, the advanced-LIGO baseline mirror radius [1]. As R increases beyond about 17 cm, $|1 - \Delta|$ increases dramatically (to about 50% when $R = 21$ cm), because for such large radii the noise *increases* (e.g. [8, 10]) with R , while the ITM scaling laws predict [Fig. 3] that the noise *always decreases* with increasing R .

When the substrate is sapphire, the FTM effects for the thermoelastic noises lead to errors that are comparable to the fused-silica FTM errors. For a mirror radius of⁶ $R = 16$ cm, the fractional error $|1 - \Delta|$ for sapphire substrates is about 15% for substrate thermoelastic noise and about 20% for coating thermoelastic noise.

⁶ When sapphire was the baseline test-mass material for advanced LIGO (it has since been abandoned in favor of fused silica), the baseline mirror radius was $R = 15.7$ cm [18].

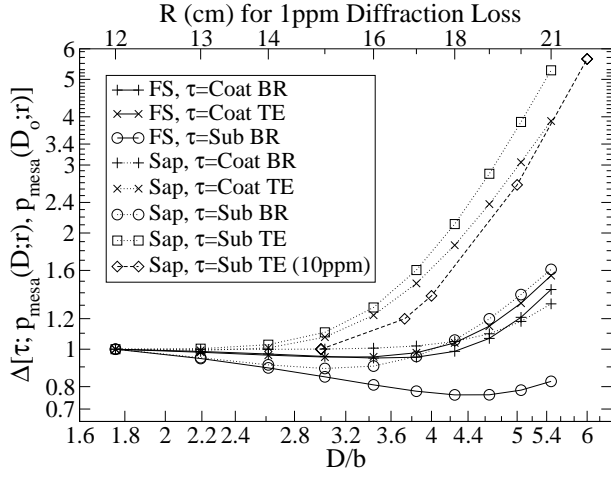


FIG. 9: A log-log plot of $\Delta[\tau; p_{\text{mesa}}(D; r), p_{\text{mesa}}(D_o; r)]$. The fractional error of the sensitivity change made by neglecting edge effects is $|1 - \Delta|$. Here the diffraction losses are 1 ppm (unless 10 ppm is indicated), and $D_o/b = 1.76$ ($D_o^{10 \text{ ppm}} = 3.00$), which corresponds to a mirror radius $R = 12$ cm ($R^{10 \text{ ppm}} = 13.94$ cm). The corresponding mirror radii are given on the top axis (1 ppm losses) and in Fig. 7 (10 ppm losses). The FTM values are obtained by taking ratios of the noises calculated by Agresti and DeSalvo [10], except for the 10 ppm values due to O'Shaughnessy, Strigin, and Vyatchanin [8]. FS and Sap mean fused-silica and sapphire substrates. (The fused-silica substrate thermoelastic noise is negligible; this case is omitted from the figure.)

2. Resized mesa beam

The FTM effects in the resized-mesa-beam case are similar to the resized-gaussian-beam FTM effects. Figure 9 plots $\Delta[\tau; p_{\text{mesa}}(D; r), p_{\text{mesa}}(D_o; r)]$. When the substrate is fused silica and $R \lesssim 17$ cm, the ITM scaling law errs by less than about 10% for the coating noises and by less than about 25% for the substrate Brownian noise. (The substrate thermoelastic noise is negligible when the substrate is fused silica [10].) Again, the ITM scaling law disagrees more and more strongly as R is increased beyond 17 cm. In this regime, the noise *increases* with R , but the ITM scaling law [Fig. 4] predicts that the noise *always decreases* with increasing R .

When the substrate is sapphire, the FTM effects for the thermoelastic noises are comparable to the Brownian-substrate errors for fused silica. When $R = 16$ cm, the FTM effects on the sapphire thermoelastic noises correspond to a fractional error $|1 - \Delta|$ of 20% – 30%.

3. Switching from a gaussian beam to a mesa beam with the same diffraction loss and mirror radius

The errors due to neglecting FTM effects in the gaussian-to-mesa case behave qualitatively differently from (and are generally smaller than) the resized-beam errors. Figure 10 plots $\Delta[\tau; p_{\text{mesa}}(D; r), p_{\text{gauss}}(w; r)]$ for

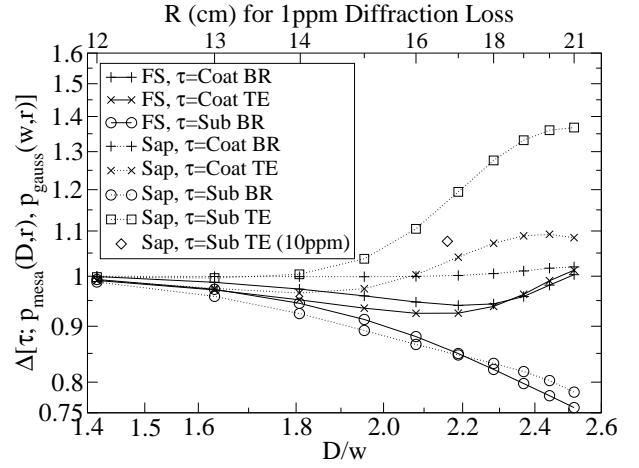


FIG. 10: A log-log plot of $\Delta[\tau; p_{\text{mesa}}(D; r), p_{\text{gauss}}(w; r)]$. The beam width parameters w and D are chosen so that the diffraction loss is 1 ppm (unless 10 ppm is indicated). The corresponding mirror width for 1 ppm diffraction losses is shown on the top axis; the 10 ppm point corresponds to a mirror radius of 15.7 cm. The fractional error of the sensitivity change made by neglecting edge effects is $|1 - \Delta|$. The FTM values are obtained by taking ratios of the noises calculated by Agresti and DeSalvo [10], except for the 10 ppm value, which is due to O'Shaughnessy, Strigin, and Vyatchanin [8]. FS and Sap mean fused-silica and sapphire substrates. (The fused-silica substrate thermoelastic noise is negligible; this case is omitted from the figure.)

fused silica and sapphire substrates. For both fused-silica and sapphire substrates, the coating sensitivity changes are not strongly sensitive to edge effects; in these cases, C_{FTM} and C_{ITM} differ by less than about 10% even when the beam widths exceed 17 cm (and thus are significant fractions of R and H [c.f. Figs. 6 and 7]). The substrate sensitivity changes are more sensitive to edge effects, but even then the edge effects remain below about 15%, provided that $R \lesssim 17$ cm for fused-silica substrates and $R \lesssim 16$ cm for sapphire substrates.

V. CONCLUSION

Changing the shape of the laser beam in advanced LIGO can reduce the thermal noise, which is the limiting noise source at frequencies from 40 Hz to 200 Hz. In the Fourier domain, the relations between the thermal noise and the beam shape for semi-infinite mirrors take the form of simple scaling laws. Moreover, the coating thermal noises obey the same local scaling law. These results enable a straightforward comparison of the thermal noises for two different beam shapes when edge effects are neglected. The scaling laws predict the improvement of mesa-beam sensitivities vs. gaussian-beam sensitivities quite well. For 40 kg, fused-silica mirrors, the substrate-noise scaling laws agree with the finite-mirror results within approximately 15% for mirror sizes not

larger than the advanced-LIGO baseline size of about 17 cm; the coating-noise scaling laws agree with the finite-mirror predictions to better than about 10%. Therefore, the infinite-test-mass scaling laws may be a very useful tool for estimating optimal beam shapes for advanced LIGO and other future gravitational-wave interferometers.

Acknowledgments

I would like to thank Kip Thorne for suggesting this problem and for his advice and encouragement. I would also like to thank Juri Agresti for helpful discussions as well as for providing for comparison the data that will be published in Ref. [10]. This work was supported in part by NSF grants PHY-0099568 and PHY-0601459. The numerical computations described in this paper were performed using *Mathematica* version 5.2. The figures, including best fit lines, were prepared using Grace 5.1.18.

APPENDIX A: A DERIVATION OF EQS. (30) AND (17)

In this appendix, I derive Eq. (30), which I use in the derivation of the scaling law for Brownian substrate noise

[Eq. (35)]. Then, I deduce Eq. (17), which I use in the derivation of the scaling law for Brownian coating noise [Eq. (22)].

First, consider the integral

$$\int_0^\infty dr r [S_{\varphi\varphi}^2 - S_{\varphi\varphi}(\theta - S_{zz})]. \quad (\text{A1})$$

Combining Eqs. (12a) and (12e) gives

$$\theta - S_{zz} = \frac{1}{2\mu} \int_0^\infty dk e^{-kz} \tilde{p}(k) \left[\frac{-\mu}{\lambda + \mu} + kz \right] k J_0(kr). \quad (\text{A2})$$

Inserting Eqs. (A2) and (12c) into the left hand side of Eq. (A1) yields

$$\int_0^\infty dr r [S_{\varphi\varphi}^2 - S_{\varphi\varphi}(\theta - S_{zz})] = \frac{1}{4\mu^2} \int_0^\infty dk \int_0^\infty dk' e^{-(k+k')z} \left[\frac{-\mu}{\lambda + \mu} + kz \right] \left[\frac{-\mu}{\lambda + \mu} + k'z \right] \tilde{p}(k) \tilde{p}(k') I, \quad (\text{A3})$$

where

$$I = \int_0^\infty dr \frac{J_1(kr) J_1(k'r)}{r} - k' \int_0^\infty dr J_1(kr) J_0(k'r). \quad (\text{A4})$$

Since k and k' are variables of integration, and since aside from I itself, Eq. (A3) is unchanged by letting $k \leftrightarrow k'$, I can be rewritten as

$$I = \int_0^\infty dr \frac{J_1(kr) J_1(k'r)}{r} - \frac{1}{2} k' \int_0^\infty dr J_1(kr) J_0(k'r) - \frac{1}{2} k \int_0^\infty dr J_1(k'r) J_0(kr). \quad (\text{A5})$$

The integrals in Eq. (A5) are special cases of Eqs. (11.4.33), (11.4.34), and (11.4.42) of Ref. [19]:

$$\int_0^\infty dr \frac{J_1(kr) J_1(k'r)}{r} = \frac{k'}{2k} \eta(k - k') + \frac{k}{2k'} \eta(k' - k), \quad (\text{A6a})$$

$$\int_0^\infty dr J_1(kr) J_0(k'r) = \frac{\eta(k - k')}{k}. \quad (\text{A6b})$$

Here η is the unit step function. Inserting Eqs. (A6a) and (A6b) into Eq. (A5) shows that

$$I = 0 \Rightarrow \int_0^\infty dr r [S_{\varphi\varphi}^2 - S_{\varphi\varphi}(\theta - S_{zz})] = 0, \quad (\text{A7})$$

which is Eq. (30).

Next, combining Eqs. (15a) – (15d) shows that

$$S_{\varphi\varphi}^{\text{coat}} = S_{\varphi\varphi}|_{z=0} \quad (\text{A8a})$$

$$\theta^{\text{coat}} - S_{zz}^{\text{coat}} = (\theta - S_{zz})|_{z=0}. \quad (\text{A8b})$$

Thus, setting $z = 0$ in Eq. (A7) gives

$$\int_0^\infty dr r [(S_{\varphi\varphi}^{\text{coat}})^2 - S_{\varphi\varphi}^{\text{coat}} (\theta^{\text{coat}} - S_{zz}^{\text{coat}})] = 0, \quad (\text{A9})$$

which is Eq. (17).

APPENDIX B: JUNCTION CONDITIONS FOR THE STRESS AND STRAIN OF A STATICALLY DEFORMED, SEMI-INFINITE MIRROR WITH THIN COATING

The junction conditions (15a) – (15d) are listed in Eq. (A4) of Ref. [4] along with the statement that for these conditions to hold, the Poisson ratios of the coating and substrate should not be “too different.” This restriction is actually unnecessary, provided that the coating is sufficiently thin. One can see this as follows:

Because the coating adheres to the substrate surface, the substrate surface and coating have the same tangen-

tial displacement. Continuity of u_r and u_φ immediately implies continuity of S_{rr} and $S_{\varphi\varphi}$. A straightforward pill-box integration of the equilibrium condition $\nabla_j T_{ij} = 0$ then shows that T_{zz} and T_{rz} are also continuous across the junction.

All of the other junction conditions given in Eq. (A.4) of Ref. [4] then follow, with one exception: the junction condition on $S_{(rz)}$ should read $\mu^{\text{coat}} S_{(rz)}^{\text{coat}} = \mu^{\text{sub}} S_{(rz)}^{\text{sub}}$, not $S_{(rz)}^{\text{coat}} = S_{(rz)}^{\text{sub}}$. But since $T_{rz} = 0$ on the coating surface (and thus also to high accuracy throughout the thin coating), this error is irrelevant; the correct junction condition is simply $S_{(rz)}^{\text{coat}} = S_{(rz)}^{\text{sub}} = 0$.

-
- [1] “Advanced LIGO: Context and Summary.” On-line document, accessed 14 September, 2006, URL <http://www.ligo.caltech.edu/advLIGO/scripts/summary.htm>.
 - [2] J. Agresti, Tech. Rep. LIGO-T040225-00-R (2005), internal LIGO document, URL <http://www.ligo.caltech.edu/docs/T/T040225-00.pdf>.
 - [3] Y. T. Liu and K. S. Thorne, Phys. Rev. D **62**, 122002 (2000).
 - [4] G. M. Harry et al., Class. Quantum Grav. **19**, 897 (2002).
 - [5] V. B. Braginsky and S. P. Vyatchanin, Phys. Lett. A **312**, 244 (2003).
 - [6] E. D’Ambrosio et al. (2004), submitted to Phys. Rev. D., URL <http://arxiv.org/abs/gr-qc/0409075>.
 - [7] E. d’Ambrosio, R. O’Shaughnessy, and K. S. Thorne, Tech. Rep. G000223-00-D (2000), internal LIGO document, URL <http://www.ligo.caltech.edu/docs/G/G000223-00.pdf>.
 - [8] R. O’Shaughnessy, S. Strigin, and S. Vyatchanin (2003), submitted to Phys. Rev. D, URL <http://arxiv.org/abs/gr-qc/0409050>.
 - [9] J. Agresti and R. DeSalvo, Tech. Rep. G050041-00-Z (2005), internal LIGO document, URL <http://www.ligo.caltech.edu/docs/G/G050041-00>.
 - [10] J. Agresti and R. DeSalvo (2005), document in preparation.
 - [11] R. O’Shaughnessy (2006), submitted to Class. Quantum Grav., URL <http://arxiv.org/abs/gr-qc/0607035>.
 - [12] S. Vyatchanin (2004), unpublished.
 - [13] J.-Y. Vinet, Class. Quantum Grav. **22**, 1395 (2005).
 - [14] Y. Levin, Phys. Rev. D **57**, 659 (1997).
 - [15] M. M. Fejer et al., Phys. Rev. D **70**, 082003 (2004).
 - [16] F. Bondu, P. Hello, and J.-Y. Vinet, Phys. Lett. A **246**, 227 (1998).
 - [17] A. E. Siegman, Opt. Lett. **1**, 13 (1977).
 - [18] P. Fritschel, Tech. Rep. T010075-00-D (2001), internal LIGO document, URL <http://www.ligo.caltech.edu/docs/T/T010075-00.pdf>.
 - [19] M. Abramowitz and I. A. Stegun, eds., *Handbook of Mathematical Functions* (Dover Publications, New York, 1964).